Energy Balance and Gas Thermalization in a High Power Microwave Discharge in N_2 - O_2 Mixtures

Samaneh Biabani and Gholamreza Foroutan*

Department of Physics, Sahand University of Technology, Tabriz, Iran

***Corresponding Author's Email:** Foroutan@sut.ac.ir

Received: Apr. 23, 2019, Revised: May. 19, 2019, Accepted: May. 22, 2019, Available Online: Dec. 27, 2019

DOI: 10.29252/ijop.13.2.155

ABSTRACT— The dynamics of fast gas heating in a high power microwave discharge in air, is investigated in the framework of FDTD simulations of the Maxwell equations coupled with the fluid simulations of the plasma. It is shown that, an ultra-fast gas heating of the order of several 100 Kelvins occurs in less than 100 ns. The main role in the heating is played by the electron impact dissociation of O_2, dissociation via quenching of metastable states of N_2, as well as, $O(^1D)$ quenching by nitrogen molecules. Among the electronically excited metastable states, $N_2(B, C, a)$ are the most important species. Slow heating of the gas above 1 μs is attributed to the vibrational relaxation processes of N_2, among them vibrational-translational relaxation of N_2 demonstrates the highest heating rate. The heating rate and thus the gas temperature are significantly increased with increasing of the microwave pulse amplitude, pulse width, and the gas pressure. In all cases, enhanced O_2 dissociation is the main factor behind the enhanced gas heating. The same effects are observed for increasing of the initial gas temperature, and O_2 percentage in a N_2 - O_2 mixture.

KEYWORDS: Microwave discharges, FDTD simulations, Fast gas heating, Gas temperature.

I. INTRODUCTION

In recent years, the study of high power microwave (HPM) discharges has attracted a lot of attention in connection with many applications including plasma assisted ignition and flame control, aerodynamic drag reduction at high speeds, sterilization of medical instruments, surface flashover in dielectric windows, design of microwave plasma jets, application in plasma propulsion technology, development of advanced radar systems, removal of nitrogen oxides from exhaust gases, generation of ozone, and purification of the earth atmosphere [1-14]. HPM discharges are characterized by a rapid enhancement of the electron number density in a short period of time of the order of a few nanoseconds. Breakdown occurs when the amplitude of the microwave pulse exceeds a critical value which depends on the pressure and gas composition. Different modes and spatial structures of the HPM discharges are observed at different gas pressures [4].

The formation of filamentary arrays due to HPM breakdown at atmospheric pressure air has been the subject of a number of recent numerical and experimental studies [15-23]. The experimental results of Hidaka *et al.* [15] and the numerical simulations by Boeuf *et al.* [17] confirm the formation of such plasma arrays. Chaudhury *et al.* [20], investigated the dynamics of microwave streamers at the antinode of two linearly polarized waves, injected in opposite directions at atmospheric pressure air with high frequency of 110 GHz under the conditions close to experiments of Hidaka [15] and Cook [21]. Their results showed that, the enhanced electric field at the head of microwave streamer causes the streamer elongation in direction parallel to the incident field, but due to the resonant effect, the streamer growth may end. Later

Kourtzanidis *et al.* [23] extended the model to 3D and studied the formation of plasma patterns during the breakdown by linear and circularly polarized waves. Their results indicated that, because of uniform elongation in the case of circular polarization, each filament is in the form of a circular disc resulting in formation of mushroom-like patterns with a distance of $\lambda/4$ between the filaments and with a propagation speed greater than that of the linearly polarized mode.

In HPM discharges at atmospheric pressure air, a major fraction of the electromagnetic energy is converted to the kinetic energy of the atoms and molecules, leading to a significant gas temperature rise. Gas heating is of crucial importance in different applications such as the plasma-assisted ignition of combustible mixtures, processing of nanomaterials, aerodynamic flow control, plasma surface treatment, the study of streamers dynamics, and control of thermal instabilities [24-32]. Gas heating in air breakdown, usually takes place in two stages: fast gas heating in a short period of time of the order of a few 100 nanoseconds, and slow heating on the time scale of milliseconds. Fast heating is related to the transfer of discharge energy into the electronic degrees of freedom of the gas molecules and then the rapid energy relaxation into translational kinetic energy. But the slow heating is due to vibrational-translational (V-T), and vibrational-vibrational (V-V) relaxation of O_2 and N_2.

In earlier studies of the plasma streamers in HPM discharges the effects of gas heating were not taken into account [20, 23]. But later Kourtzanidis *et al.* [32] studied the effects of gas heating on the microwave streamer dynamics at 110 GHz in atmospheric pressure air using the Maxwell's equations coupled to the plasma fluid model and gas dynamics equations (Euler equations). They observed the formation of a shock wave due to fast gas heating which modifies the density distribution and the ionization-diffusion mechanism in the microwave streamer and tends to limit the elongation of streamer due to enhanced resonant effects. The experimental results obtained by Schaub *et al*. [33] for a focused microwave beam at 110 and 124.5 GHz in air, showed good agreement with the numerical simulations of Kourtzanidis *et al.* [32]. They found that, gas heating reduces the density of neutral gas to more than 80% where the plasma density reaches its maximum.

Due to the importance of gas heating for various applications, numerous research works have been devoted to the study of the dynamics of heat release in air plasmas [32, 34-39, 48-52]. Popov developed a model of rapid gas heating in nitrogen-oxygen mixture by considering the dissociation of oxygen molecules by direct electron impact and via quenching of the electronically excited nitrogen molecules. It was shown that the fraction of the discharge power, expended on the excitation of electronic degrees of freedom of molecules, is fixed in a wide range of the reduced electric field, E/N. A lower fractional concentration of oxygen molecules in the mixture leads to a smaller fraction of the energy of excited electronic degrees of freedom which is spent on gas heating [35]. Later, Popov presented the dependence of the rates of different processes involved in the fast heating on the reduced electric field in a significantly wide range. It was shown that, for $E/N > 400$ Td (10^{-17} Vcm^2), the fast gas heating is mainly due to the electron impact dissociation of N_2 molecules and the processes involving charged particles. For $E/N \le 200$ Td, the dissociation of oxygen molecules by electron impact and quenching of electronically excited nitrogen molecules and also the quenching of excited $O(^1D)$ atoms by nitrogen molecules are the most important processes in the gas heating [37].

The dynamics of fast gas heating has also been studied experimentally by different research groups [24, 25, 33, 40-47]. Aleksandrov *et al.* [40] investigated the mechanism of electron energy transfer into ultrafast gas heating in air plasma at high electric fields, both for a high-voltage nanosecond discharge and surface

dielectric barrier discharge. They found that, at high electric field of 10^3 Td, approximately half of the discharge energy is converted into heat for a short period of time of the order of 1 μs. Later Rusterholtz *et al.* [41] presented a detailed experimental study of the ultrafast heating in a nanosecond repetitively pulsed discharge, produced between pin-to-pin electrodes with distance of 4 mm, and pulses of amplitude of 5.7 kV, duration of 10 ns, and repetition frequency of 10 kHz, in preheated air at atmospheric pressure. The ultrafast heating leads to electronic excitation of nitrogen molecules which in turn dissociate O_2 molecules via quenching reactions with the remaining energy going into gas heating. They showed that about 50% of molecular oxygen is dissociated and the gas temperature is increased about $\Delta T = 900$ K in 20 ns, indicating an ultrafast heating rate of about $5\times10^{10}\,\mathrm{Ks}^{-1}$.

The slow gas heating in air discharges occurs on the time scale of ms or longer and is mainly attributed to vibrational relaxation of N_2 molecules including V-V exchanges between nitrogen molecules and V-T relaxation in $N_2 - N_2$, $N_2 - O_2$, $N_2 - N$, and $N_2 - O$ reactions [49-52]. In [52], a time-dependent model of gas heating with a complete set of gas heating mechanisms in N_2 and $N_2 - O_2$ plasmas was presented. The model also considers the energy transfer via V-V and V-T exchanges of N_2 for much longer times of 10^2 ms. The simulation results showed that for a constant value of the reduced electric field E/N, and the electron number density, the total gas heating rate and also the gas temperature are increased with increasing of the fractional concentration of oxygen molecule in the $N_2 - O_2$ mixture.

In a previous work, we presented a self-consistent numerical model to study the diffusive mode of a HPM discharge in air and investigated the effects of variation in different parameters, such as the gas pressure, the width, frequency and amplitude of the microwave pulse on the properties of the plasma and evolution of the concentrations of the electrons, ions and radicals [53]. For the conditions considered there, the energy absorbed by the electrons from the wave field, was very high and as a result, the electron energy is effectively transferred into electronic states of the gas molecules and then to fast gas heating. On the other hand, the fast gas heating significantly affects the rates of different gas phase reactions and consequently the dynamics of radicals and charged particles. In that work we briefly discussed the effects of temperature increase on the evolution of the number densities of electrons, O, NO, $N_2(A)$, $N_2(B)$, and $N_2(C)$, without presenting a detailed calculations model for fast gas heating. On the other hand, there are few studies on the effects of different control parameters on the gas heating in HPM discharges. In this work, we present a numerical model of fast gas heating in a HPM discharge in air, and investigate the effects of gas parameters and the properties of microwave source on the heating rate, gas temperature and evolution of radicals and plasma particles. To this end, we study the effects of variation in the air pressure, initial gas temperature, oxygen percentage, and the amplitude and duration of the microwave pulse on the heating rate and gas temperature for a single pulse with the total simulation time of about 10 μs. Instead of listing an exhausted set of all chemical reactions, we only present the most important reactions involved in the fast gas heating.

The structure of the paper is as follows: Section II presents the theoretical model including the equations describing the propagation of microwave pulse and evolution of the plasma parameters and gas temperature, as well as the chemistry model and the associated data set. Section III provides the results of numerical simulations along with a detailed discussion of different effects, and compares them with the available results in the literature. Finally, the paper is concluded in Section IV with a summary of the main findings.

II. THEORETICAL MODEL

In this section, we address the theoretical model used in the simulation of the HPM pulse. The finite-difference time domain (FDTD) method has been extensively used to obtain the numerical solutions of the Maxwell equations in conjunction with the fluid equations describing the evolution of the plasma particles [13, 14, 17-20, 23, 32]. In the following we first introduce the Maxwell equations along with the electron fluid equations and then briefly discuss the chemical model of the discharge with focusing on the most important reactions in the gas heating.

A. *Maxwell Equations and Plasma Dynamics*

The one-dimensional Maxwell equations for propagation of a microwave pulse through the plasma along z direction are given as [13]:

$$\frac{\partial E_x}{\partial t} = -\left(\frac{1}{\varepsilon_0}\right)\frac{\partial H_y}{\partial z} - \frac{q_e N_e u_x}{\varepsilon_0}, \quad (1)$$

$$\frac{\partial E_z}{\partial t} = -\frac{q_e N_e u_z}{\varepsilon_0}, \quad (2)$$

$$\frac{\partial H_y}{\partial t} = -\left(\frac{1}{\mu_0}\right)\frac{\partial E_x}{\partial z}, \quad (3)$$

where E_x and E_z are the x and z components of the electric field, H_y is the y component of the magnetic field. q_e and N_e are the electron charge and number density, u_x and u_z are the mean electron velocity components along x and z directions, ε_0 and μ_0 denote the permittivity and permeability of free space.

In fluid approach the electron dynamics is described by the continuity, momentum and energy equations [13]:

$$\frac{\partial N_e}{\partial t} = (\nu_i - \nu_a) N_e - \frac{\partial (N_e u_z)}{\partial z}, \quad (4)$$

$$\frac{\partial (N_e u_x)}{\partial t} = \frac{q_e}{m_e} N_e E_x - \frac{q_e}{m_e} N_e \mu_0 u_z H_y - \nu_c N_e u_x, \quad (5)$$

$$\frac{\partial (N_e u_z)}{\partial t} = \frac{q_e}{m_e} N_e E_z + \frac{q_e}{m_e} N_e \mu_0 u_x H_y - \nu_c N_e u_z - \frac{1}{m_e}\frac{\partial (N_e \bar{\varepsilon}_e)}{\partial z}, \quad (6)$$

$$\frac{\partial (N_e \bar{\varepsilon}_e)}{\partial t} = q_e (N_e u_x E_x + N_e u_z E_z) - N_e Q_l, \quad (7)$$

where, m_e is the electron mass, $\bar{\varepsilon}_e$ is the mean electron energy. ν_i, and ν_a are the ionization and attachment frequencies for the electrons, ν_c is the momentum transfer collision frequency, and Q_l is the electron energy loss rate in collisions (elastic and inelastic). The ionization, attachment, and momentum transfer collision frequencies as well as the electron energy loss rate are calculated using BOLSIG+ software [54].

The temporal evolution of the gas temperature under isobaric conditions can be written as [50]:

$$n_m c_p \frac{\partial T_g}{\partial t} = \lambda_g \nabla^2 T_g + Q_{in}, \quad (8)$$

where n_m and c_p denote the molar density and the molar heat capacity at constant pressure, λ_g is the thermal conductivity, and Q_{in} is the total rate of gas heating in the exothermic reactions considered, for example:

$$\mathrm{A} + \mathrm{B} \rightarrow \mathrm{C} + \mathrm{D}, \quad (9)$$

$$Q_{in} = \mathrm{N_A N_B} k \Delta E, \quad (10)$$

where, N_i denotes the number density of species i, k is the rate constant, and ΔE is the energy released during the reaction.

B. *Chemical Kinetics*

In the chemical model presented here, we mainly focus on the most important species

and chemical reactions involved in fast gas heating.

Table 1. The reactions included in the gas heating, the corresponding rate coefficients and energies converted on gas heating. T_e and T are the electron temperature in Volts and gas temperature in Kelvins, respectively.

No.	Reaction	Rate constant $\left(\mathrm{cm^3 s^{-1}}\right)$	$\Delta E\,(\mathrm{eV})$	Reference
1	$e + O_2 \rightarrow e + O + O$	$f(T_e)$	0.8	[54]
2	$e + O_2 \rightarrow e + O + O(^1D)$	$f(T_e)$	1.26	[54]
3	$e + N_2 \rightarrow e + N + N(^2D)$	$f(T_e)$	0.9	[54]
4	$N_2(A) + O_2 \rightarrow N_2(X) + O + O$	2.54×10^{-12}	1.05	[55]
5	$N_2(A) + N_2(A) \rightarrow N_2(B) + N_2(v=2)$	7.7×10^{-11}	4	[49]
6	$N_2(A) + N_2(A) \rightarrow N_2(C) + N_2(v=2)$	1.5×10^{-10}	0.4	[49]
7	$N_2(A) + O(^3P) \rightarrow NO + N(^2D)$	7.0×10^{-12}	0.5	[55]
8	$N_2(B) + O_2 \rightarrow N_2(X) + O + O$	3.0×10^{-10}	2.23	[49]
9	$N_2(B) + N_2 \rightarrow N_2(A) + N_2$	2.85×10^{-11}	1.18	[49]
10	$N_2(B) + O(^3P) \rightarrow NO + N(^2D)$	3.0×10^{-10}	1.74	[38]
11	$N_2(C) + O_2 \rightarrow N_2(X) + O + O$	3.0×10^{-10}	5.91	[49]
12	$N_2(C) + O(^3P) \rightarrow NO + N(^2D)$	3.0×10^{-10}	5.42	[38]
13	$N_2(a') + O_2 \rightarrow N_2(X) + O + O$	2.8×10^{-11}	3.28	[49]
14	$N_2(a') + O(^3P) \rightarrow NO + N(^2D)$	3.0×10^{-10}	2.79	[38]
15	$N_2(a) + O_2 \rightarrow N_2(X) + O + O$	4.3×10^{-10}	3.43	[49]
16	$N_2(w) + O_2 \rightarrow N_2(X) + O + O$	1.0×10^{-10}	3.77	[49]
17	$N(^2D) + N_2 \rightarrow N(^4S) + N_2$	6.0×10^{-15}	2.38	[55]
18	$N(^2D) + O_2 \rightarrow NO + O(^1D)$	$6.0\times10^{-12}\,(T/300)^{0.5}$	1.76	[55]
19	$N(^2D) + O_2 \rightarrow NO + O(^3P)$	$1.5\times10^{-12}\,(T/300)^{0.5}$	3.73	[55]
20	$N(^2D) + O(^3P) \rightarrow N(^4S) + O(^3P)$	1.8×10^{-12}	2.35	[38]
21	$N(^2P) + N_2 \rightarrow N(^4S) + N_2$	2.0×10^{-18}	3.58	[56]
22	$O(^1D) + N_2 \rightarrow O(^3P) + N_2$	$1.8\times10^{-11}\exp(107/T)$	1.38	[55]
23	$O(^1D) + O_2 \rightarrow O(^3P) + O_2$	$6.4\times10^{-12}\exp(67/T)$	1.38	[56]
24	$O(^1D) + O_2 \rightarrow O(^3P) + O_2(b^1\Sigma_g^+)$	$2.56\times10^{-11}\exp(67/T)$	0.33	[55]
25	$O(^1D) + NO \rightarrow O(^3P) + NO$	1.7×10^{-10}	1.97	[38]
26	$O(^1D) + O(^3P) \rightarrow O(^3P) + O(^3P)$	8.0×10^{-12}	1.97	[56]
27	$O(^1S) + O(^3P) \rightarrow O(^1D) + O(^3P)$	$5.0\times10^{-11}\exp(-301/T)$	2.22	[55]
28	$O(^1S) + NO \rightarrow O(^3P) + NO$	2.9×10^{-10}	4.19	[56]
29	$O(^1S) + NO \rightarrow O(^1D) + NO$	5.1×10^{-10}	2.22	[56]
30	$O_2(b^1\Sigma_g^+) + O(^3P) \rightarrow O(^3P) + O_2(a^1\Delta_g)$	8.0×10^{-14}	0.65	[55]
31	$N(^4S) + NO \rightarrow N_2(v\sim3) + O(^3P)$	$1.05\times10^{-12}T^{0.5}$	2.45	[52]
32	$N(^4S) + NO \rightarrow N_2(v=4,5) + O(^3P)$	3.0×10^{-11}	2.45	[38]

We consider 31 different species, including the excited states of the molecular and atomic nitrogen and oxygen $N_2(\nu_i, i=1,...,8)$, $N_2(A\,^3\Sigma_u^+, B\,^3\Pi_g, C\,^3\Pi_u, a'\,^1\Sigma_u^-, a\,^1\Pi_g, w\,^1\Delta_u)$, $O_2(a\,^1\Delta_g, b\,^1\Sigma_g^+)$, $O(^1D, ^1S)$, $N(^2D, ^2P)$, as well as the neutral species $O, O_2, O_3, N, N_2, NO, NO_2, N_2O, NO_3, N_2O_5$, besides electrons. 278 different chemical reactions including electron impact reactions, V-T relaxations, V-V exchanges and reactions involving neutrals in N_2 and O_2 mixture are included in the model.

The set of the most important chemical reactions in the gas heating is given in Table 1. Our chemical model also takes into account the heating arising from V-T relaxation in $N_2 - N_2$, $N_2 - N$, $N_2 - O$, and V-V energy exchange in $N_2 - N_2$. We have used BOLSIG+ free software to calculate the rates of ionization, electron impact dissociation and excitation of the particles, due to their dependence on the electron temperature [54]. The reduced electric field E/N is an important factor in determining the contribution of different reactions in fast gas heating. According to Ref. [37], for $E/N < 200$ Td (1 Td=10^{-17} V cm^2) in air, electron impact dissociation of O_2 as well as the dissociation via quenching of the electronically excited nitrogen molecules, along with $O(^1D)$ quenching by N_2 are the most important processes in the fast gas heating:

$$e + O_2 \rightarrow e + O + O(^3P, ^1D), \quad (11)$$

$$N_2(A, B, C, a, a', w) + O_2 \rightarrow N_2 + 2O, \quad (12)$$

$$O(^1D) + N_2 \rightarrow O(^3P) + N_2, \quad (13)$$

where, the energy converted to gas heating in processes (11) and (12) can be directly obtained from the difference between the threshold energies for excitation of N_2 and O_2 molecules and the dissociation energy of the products, which is 7.08 eV for producing $O(^3P) + O(^1D)$ and 5.12 eV for $O(^3P) + O(^3P)$.

In reaction of the excited species, part of the released energy may go to vibrational excitation of the products, but we have assumed that, in most of the exothermic reactions considered in this work, all of the released energy is converted to gas heating. In reaction (13) about 70% of the released energy is spent on gas heating that is equal to 1.38 eV.

The electron impact dissociation of nitrogen molecules

$$e + N_2 \rightarrow e + N(^4S) + N(^2D), \quad (14)$$

also contributes to fast gas heating with an energy ≤ 1 eV. Other chemical processes, important in fast gas heating are:

$$N_2(a', B, C) + O(^3P) \rightarrow NO + N(^2D), \quad (15)$$

$$N(^2D) + O_2 \rightarrow NO + O(^3P, ^1D) \quad (16)$$

Due to large increase in the atomic oxygen density during breakdown, the following V-T relaxation:

$$N_2(\nu) + O(^3P) \rightarrow N_2(\nu\text{-}1) + O(^3P), \quad (17)$$

is the most important process among the relaxation reactions of vibrationally excited states of N_2 in $N_2 - O_2$ mixtures, but the contribution of this process in the fast gas heating is much less than processes (11)-(16).

III. NUMERICAL RESULTS AND DISCUSSION

For numerical simulation of the model equations, FDTD method is used to discretize the Maxwell Eqs. (1)-(3). At the same time CPML (convolutional perfectly matched layer) boundary condition is applied to update the field components at the boundaries of the

simulation domain. Also, the fluid Eqs. (4)-(7) are solved by explicit Euler scheme. Moreover, Eq. (8) is solved along with the rate equations for the neutral species to update the gas temperature and the number densities of the neutrals. The numerical stability condition required by the FDTD method is the CFL condition

$$\Delta t \le \frac{\Delta z}{c}, \tag{18}$$

where, c is the speed of light in free space. The computational domain in this simulation is 20 cm in air. Modulated Gaussian microwave pulses are injected from the left boundary and the default values for the microwave pulses are: frequency f=2.85 GHz, pulse width τ_p=30 ns, electric field amplitude E_0=10 MV/m, and the initial gas temperature T=300 K. It was assumed that the number densities of N_2 and O_2 are fixed and do not change during the discharge. Because of the symmetry in the spatial and temporal profiles, we only present the time evolution of different quantities at a given position (z =0.07 m).

First, we study the time evolution of the number densities of the main species involved in the gas heating during a microwave pulse. This can be used to explain the contribution of different reactions in the heating rate and thus in the gas temperature rise. During the discharge pulse, the electron number density (not shown) rises very quickly, then as seen from Fig. 1, the number densities of the excited $N_2(A, B, C, a, a', w)$, and $N(^2D, ^2P)$, and $O(^1D, ^1S)$ states are increased as a result of electron impact excitation from the ground state. Also, the concentrations of N and O are increased due to the electron impact dissociation processes.

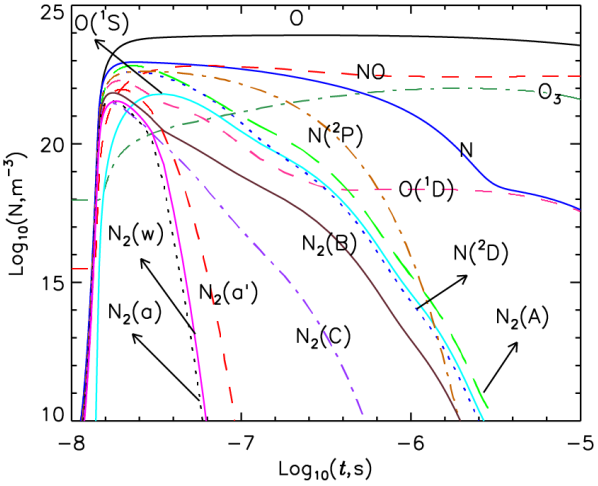

Fig. 1. Time evolution of the concentrations of the most important radicals and excited species involved in gas heating for a microwave pulse with amplitude of 10 MV/m, duration of 30 ns, propagating in air with initial temperature of 300 K, and pressure of 760 Torr.

Because of its lower excitation energy, $N_2(A)$ is more populated than the other metastable states of nitrogen molecule. This reason is also true for $O(^1D)$ compared to $O(^1S)$. After the discharge pulse, the concentrations of the excited species decrease both due to decrease in the electron number density and quenching by oxygen and nitrogen molecules.

To scrutinize the contribution of different processes in gas heating we study the time evolution of the heating rate for the most important exothermic reactions. For the source parameters considered in this work, the mean value of the reduced electric field is less than 200 Td. Therefore, as shown in Fig. 2, electron impact dissociation of O_2 and dissociation via quenching of the electronically excited nitrogen molecules, as well as $O(^1D)$ quenching by N_2 are the most important reactions in the fast gas heating. These are in good agreement with the results of Popov [37].

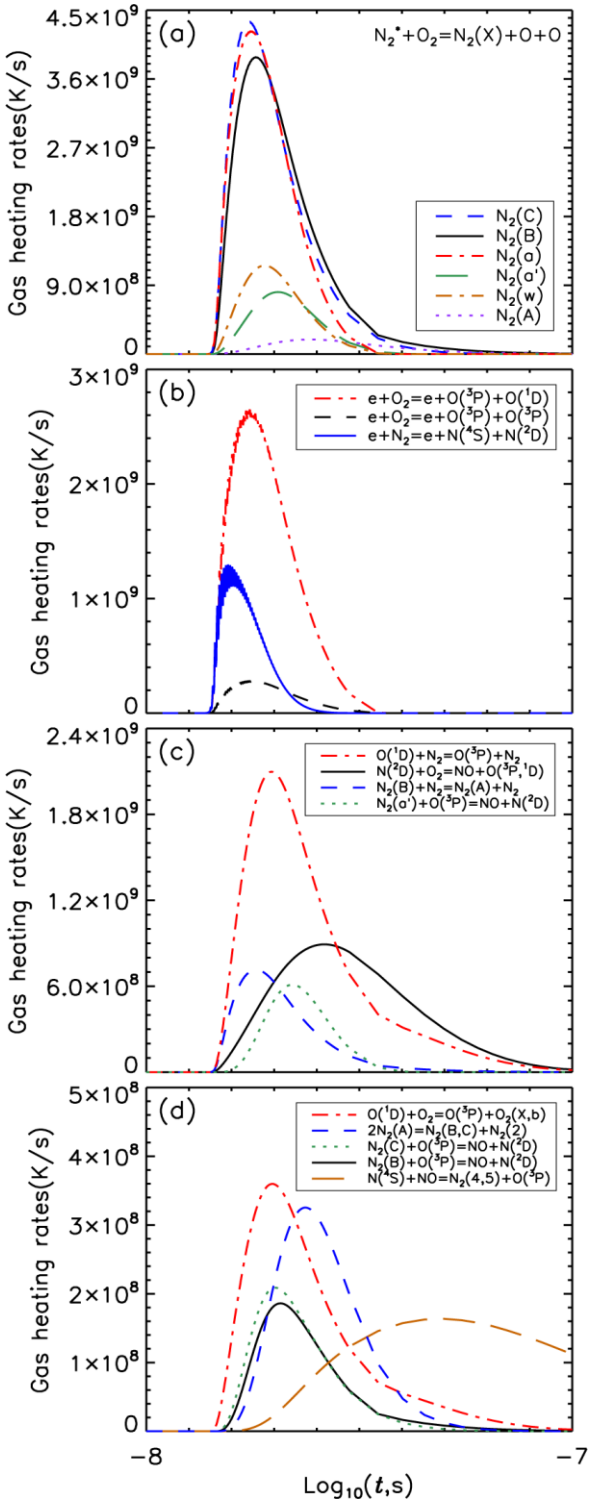

Fig. 2. The time evolution of the heating rates of different reactions for the same microwave pulse parameters and air conditions as in Fig. 1.

Figure 2(a) compares different channels of O_2 dissociation by different electronically excited states of nitrogen molecules. It is obvious that $N_2(C)$, $N_2(B)$, and $N_2(a)$ have more contribution than the other three excited states. This is related to the higher rate constant and higher energy release in these reactions. Although, according to Fig. 1, the peak number density of $N_2(A)$ is higher than that of the other electronically excited states, but the associated rate constant times the energy spent on gas heating is much lower. The contribution of the electron impact dissociation channels in gas heating, depends on the rate constant, the electron number density, and the amount of energy released as heat. Due to rapid increasing of the electron number density during the breakdown, these processes are very important in HPM discharges, as is clear from Fig. 2(b). The reaction $e + O_2 \rightarrow e + O + O(^1D)$, has a higher heating rate compared to the other two reactions due to its higher rate constant and larger heat release. The other important channels in the gas heating, are shown in Figs. 2(c) and 2(d). Because of high concentrations of $O(^1D)$ and N_2, and also a larger rate constant compared to the other reactions, the process (13) has a significant contribution in the gas heating.

Time evolution of the population of the 8 lowest excited vibrational states of N_2 and the associated heating rates in different relaxation processes, are presented in Fig. 3. The highest heating rate among these processes belongs to $N_2 - O$ vibrational-translational relaxation with the maximum of $4.7\times10^7\,Ks^{-1}$. $N_2 - N$ vibrational-translational relaxation is an important process for small times of the order of hundreds of nanoseconds while V-V $N_2 - N_2$ overcomes above microseconds. Vibrational-Translational relaxation of $N_2 - N_2$ plays little role in the gas heating among the vibrational processes. From comparison of Figs. 2 and 3, we find that the gas heating at times t<1 μs is mainly due to O_2 dissociation processes by electron impact and quenching of electronically excited species of N_2, while for times above 1 μs the vibrational relaxation of N_2 molecules plays

the main role in the heating. It is noted that, the population of vibrational levels of N_2, increases with decreasing of the vibrational number.

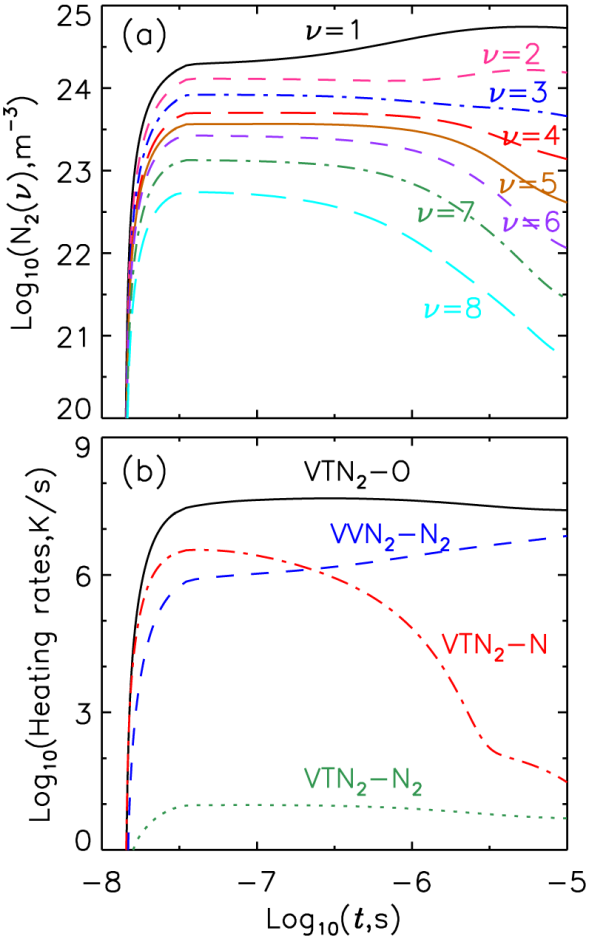

Fig. 3. Temporal evolution of the population, and the associated heating rates of different vibrational levels of N_2 for the same conditions as in Fig. 1.

To investigate the effects of different control parameters on the heating rate and gas temperature, we first study the effects of variation in the pulse amplitude. Figure 4 shows the time evolution of the total heating rate and the gas temperature for four different amplitudes of the pulse electric field. The gas temperature increases in two different stages: an increase on the order of a few hundreds Kelvins in less than 100 nanoseconds and then an increase after t=1 μs. For default field amplitude of E_0=10 MV/m in the Fig. 4, the heating starts after 15 ns, when the pulse amplitude reaches its maximum and the heating rates associated with the dissociation processes (11) and (12) become high enough to increase the gas temperature. The gas heating after t=1 μs is due to vibrational relaxation of N_2 molecules, among them the most important process in air is V-T $N_2 - O$, as seen from Fig. 3. For E_0=10 MV/m the gas temperature reaches 960 K at t=10 μs with the corresponding total heating rate peaking at t=30 ns with a maximum value of 2.2×10^{10} Ks^{-1}.

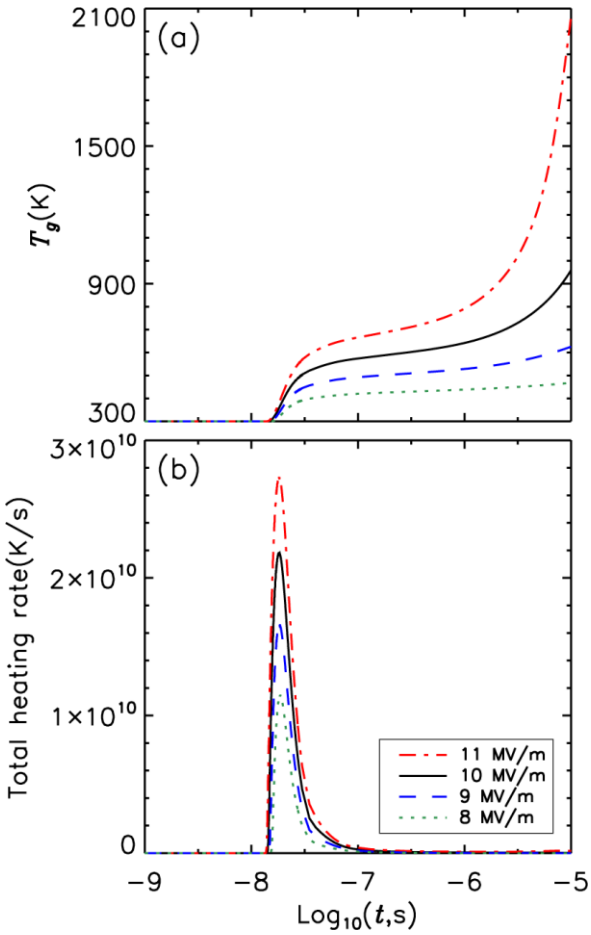

Fig. 4. Time evolution of the gas temperature and the total heating rate for different amplitudes of the pulse electric field.

These are in good agreement with the results of [38]. With increasing of the pulse amplitude, the electron number density and the mean electron energy are increased and as a result the rates of electron impact dissociation processes are enhanced. This in turn results in increasing of the number densities of the vibrational and electronically excited species

of N_2 and O_2 and hence in increasing of the corresponding heating rates.

Figure 5 represents the time dependence of the gas temperature, the total heating rate, and the number density of atomic oxygen for four different values of the pulse width τ_p.

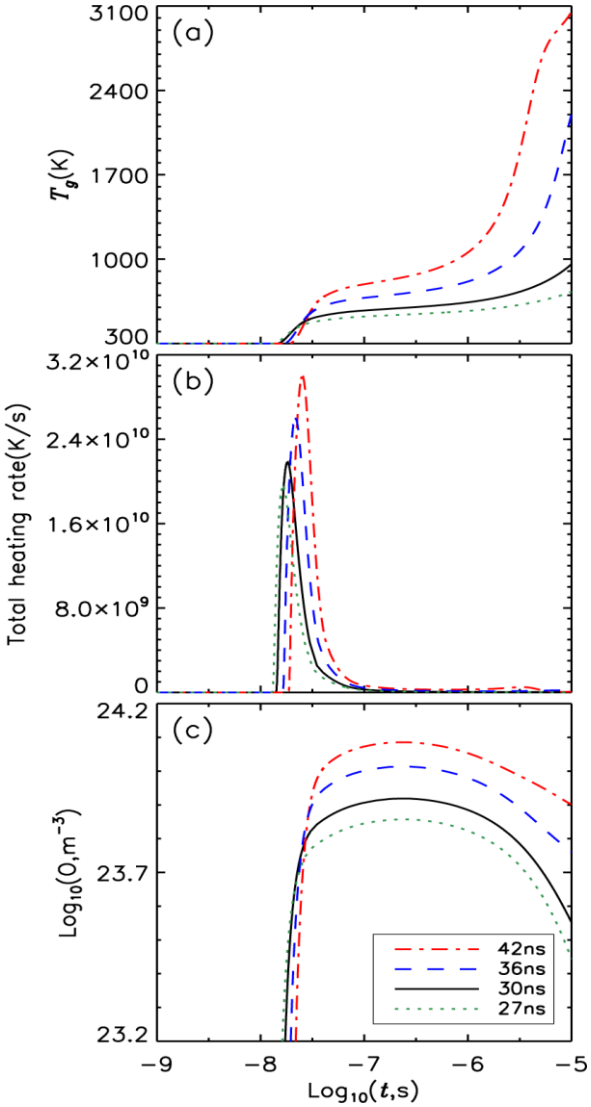

Fig. 5. Time dependence of (a) the gas temperature, (b) the total heating rate, and (c) the number density of atomic oxygen for four different values of the pulse width.

It is clearly seen from Fig. 5 that, with increasing of τ_p, the total heating rate and the gas temperature are increased. For long pulse widths, more electric energy is transferred to the electrons and thus the electron number density and the mean electron energy are enhanced. This results in more electron impact dissociation of O_2 and also in enhanced electronic excitation of N_2 molecules which take part in the O_2 dissociation as well. Therefore, the heating rate and the gas temperature are increased with increasing of τ_p. Enhanced dissociation of O_2 molecules at longer pulse durations leads to higher concentration of atomic oxygen, as seen from Fig. 5(c). Higher O number density, in turn accelerates the V-T N_2 - O relaxation and thus leads to a larger heat release and thus to a higher gas temperature.

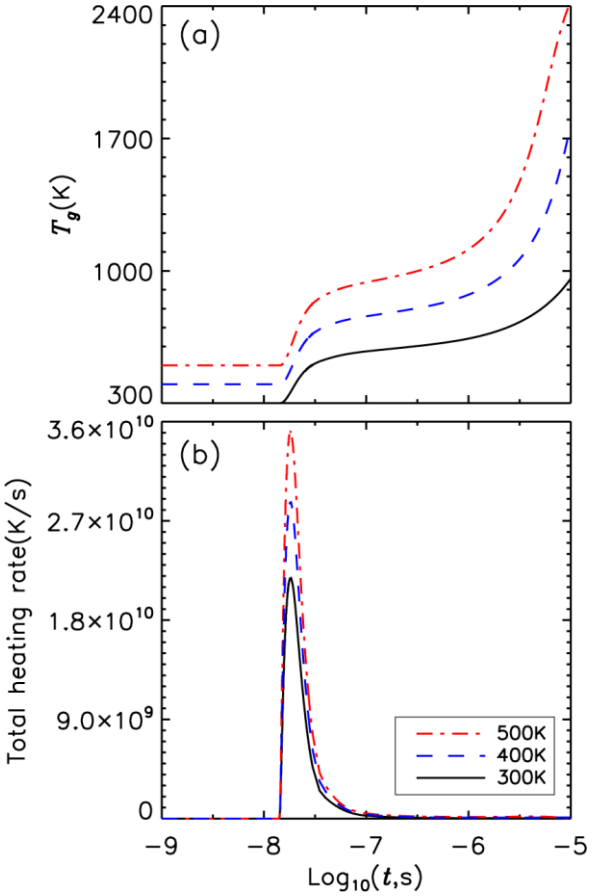

Fig. 6. Time evolution of the gas temperature and the total heating rate for three different values of the initial gas temperature.

Now we study the effects of gas parameters on the dynamics of fast gas heating. Figure 6 displays the time evolution of the total heating rate and the gas temperature for three different initial gas temperatures. Although, the rate constants for the electronically excited states involved in the gas heating as well as that of the electron impact reactions do not depend on

the gas temperature, but some processes are still, like reactions 18, 19, 27, and 31 in Table 1, which are accelerated with increasing of the gas temperature. This leads to a higher gas heating rate, as seen from Fig. 6(b). For an initial gas temperature of 500 K, the peak heating rate increases to $3.5\times10^{10}\,\mathrm{Ks^{-1}}$ compared to $2.2\times10^{10}\,\mathrm{Ks^{-1}}$ for 300 K. The ratio of the final gas temperatures is 2.5.

Due to the importance of O_2 dissociation in the heat release, we investigate the effects of variation in O_2 percentage on the heating dynamics in a HPM discharge in N_2-O_2 mixture. Figure 7 displays the heating rate, the gas temperature, and O atom concentration for five different O_2 percentages. The heating rate and the gas temperature are increased with increasing of the oxygen population. For instance, with increasing of O_2 population from 21% to 80% the final gas temperature is doubled. The electron impact dissociation of O_2 as well as the dissociation via electronically excited N_2 molecules are enhanced which in turn lead to more heat release and thus to increasing of the gas temperature. Enhanced O_2 dissociation also results in enhanced atomic oxygen population as is clear from Fig. 7(c). Atomic oxygen can then participate in numerous heating processes such as reactions 10, 12, 14, and 20 in Table 1. Moreover for $t>1\ \mu s$, due to increasing of O number density with O_2 percentage, the heating rate of V-T N_2-O reaction is enhanced which in turn leads to more gas heating. Further increasing of O_2 population above 80%, leads to a saturation in the gas temperature. This is attributed to the reduction in the N_2 population, as less electronically excited N_2 molecules are available to dissociated O_2 and release heat.

Finally, we explore the effects of gas pressure on the fast gas heating. Figure 8 represents the gas temperature, the total heating rate, $N_2(C)$ concentration, and O atom number density for five different gas pressures. As is obvious, the heating rate and the gas temperature are increased with increasing of the pressure.

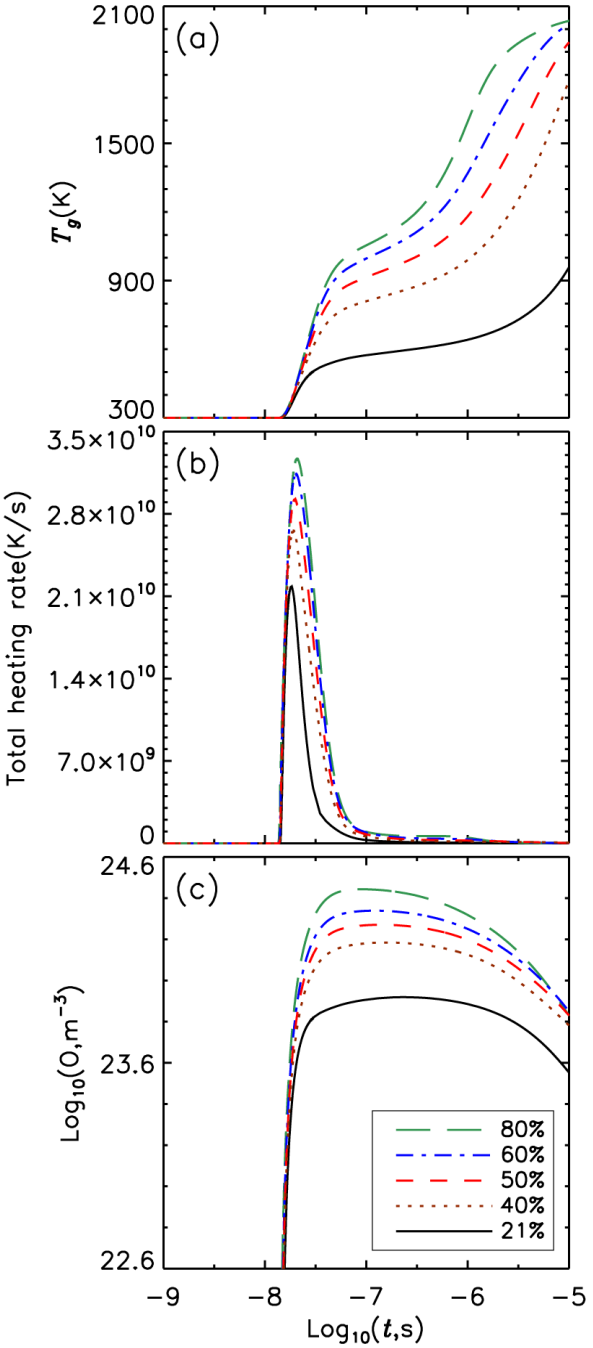

Fig. **7.** The gas temperature, the total heating rate, and the number density of atomic oxygen as functions of time for five different O_2 percentages**.**

This effect can be explained in terms of the enhanced collision frequency at higher gas pressures. With increasing of the collision frequency, the electron impact dissociation of O_2 as well as the dissociation via electronically excited N_2 molecules are

enhanced. Then, as shown in Fig. 8(d), the O atom number density increases.

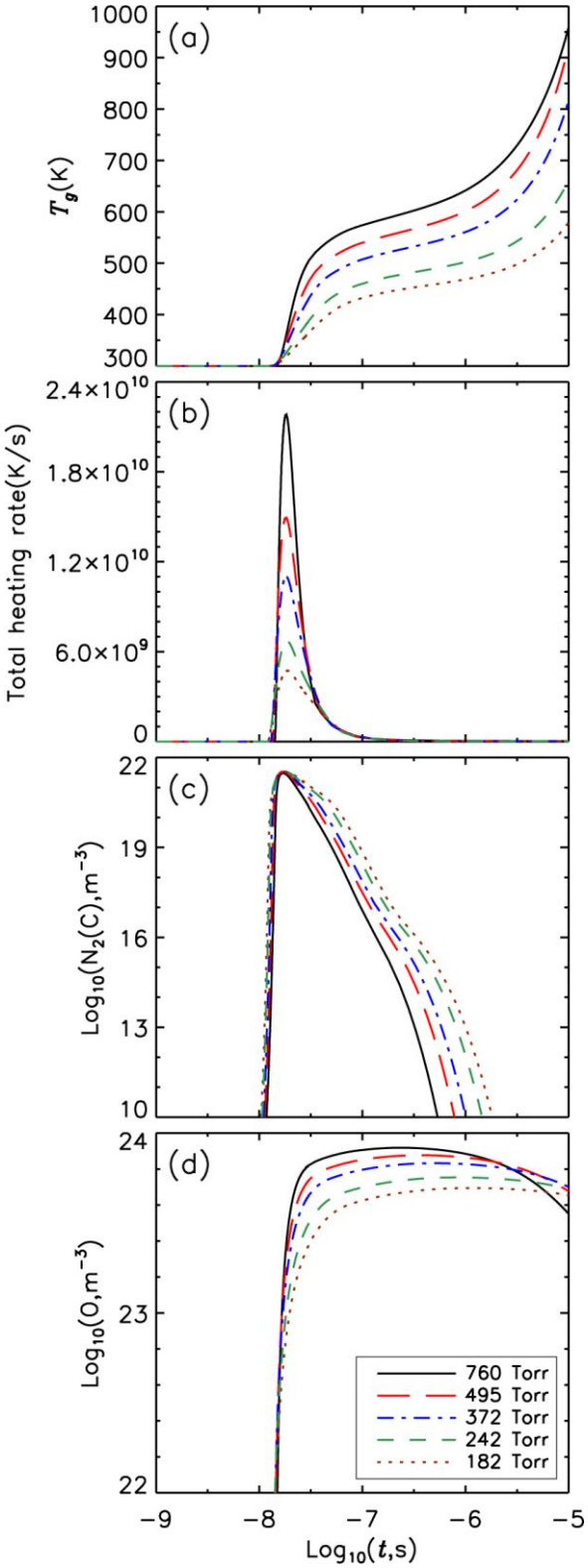

Fig. 8: The gas temperature, the total heating rate, and the concentrations of atomic oxygen and $N_2(C)$ as functions of time for five different pressures.

On the other hand, due to more frequent collisions at higher pressures, electronically excited metastable states of N_2 are effectively consumed in O_2 dissociation process. Then, as seen from Fig. 8(c), the concentrations of $N_2(C)$ and the other metastable states (not shown) are reduced. Enhanced O_2 dissociation along with higher O atom number density results in more heat release and thus to increasing of the gas temperature.

IV. CONCLUSION

We studied the process of fast gas heating in a HPM discharge at atmospheric pressure air. We presented a self-consistent numerical model by coupling the FDTD simulation of Maxwell equations with fluid description of the plasma and investigated the effects of different control parameters such as air pressure, initial gas temperature, oxygen percentage, the microwave pulse amplitude, and the pulse width on the heating rate and gas temperature. The main results of the simulation are summarized as follows:

The concentrations of electrons and the excited species of atoms and molecules are increased in a short period of time in the order of a few nanoseconds. Then the electron impact dissociation of oxygen molecules and dissociation via quenching of electronically excited nitrogen molecules, as well as $O(^1D)$ quenching by N_2 lead to fast gas heating of a few 100 Kelvin in less than 100 ns. The next phase of gas heating, the so called slow heating, occurs above 1 μs second and is attributed to the vibrational relaxation of N_2 molecules. Among the metastable states of N_2, the most important species in gas heating are $N_2(B, C, a)$, while $N(^2D, ^2P)$ and $O(^1D, ^1S)$ are the most important atomic species. The highest heating rate among vibrational relaxation processes of N_2, belongs to $N_2 - O$ V-T relaxation.

The heating rate and consequently the gas temperature are increased with increasing of the microwave pulse width and amplitude. This is because, at higher pulse amplitude and duration, more electromagnetic energy is transferred to the electrons. Then the electron number density and mean electron energy are increased. This in turn leads to more O_2 dissociation both by direct electron impact and via quenching of the metastable states of N_2. The energy released during these O_2 dissociation processes is converted to heat and results in increasing of the gas temperature. On the other hand, higher dissociation leads to higher atomic oxygen concentration which can participate in different heating reactions like V-T $N_2 - O$ relaxation.

Increasing of the pressure and the percentage of O_2 in a N_2- O_2 mixture has similar effects. At higher gas pressures the collision frequency of electrons with neutral is increased. Then O_2 dissociation by direct electron impact is enhanced. On the other hand, due to more frequent collisions, metastable states of N_2 can effectively dissociate O_2 molecules. The higher O_2 dissociation, corresponds to more heat release and thus to higher gas temperature. O_2 dissociation also increases with increasing of O_2 percentage up to 80%. At higher O_2 percentage, less metastable N_2 is available to dissociate O_2. Moreover, the contribution of vibrational relaxation of N_2 in the gas heating diminishes. As the rate constant of some of the reactions involved in gas heating depends on the gas temperature, the heating rate and the gas temperature are enhanced with increasing of the initial gas temperature.

V. REFERENCES

[1] A.D. MacDonald, *Microwave Breakdown in Gases (John Wiley & Sons)*, New York, 1966.

[2] D. Anderson, M. Lisak, and T. Lewin, "Breakdown in air-filled microwave waveguides during pulsed operation," J. Appl. Phys. Vol. 56, pp. 1414-1419, 1984.

[3] D. Knight, "Survey of Aerodynamic Drag Reduction at High Speed by Energy Deposition," J. Propul. Power, Vol. 24, pp. 1153-1167, 2008.

[4] K.V. Khodataev, "Microwave Discharges and Possible Applications in Aerospace Technologies," J. Propul. Power, Vol. 24, pp. 962-972, 2008.

[5] K.V. Aleksandrov, V.L. Bychkov, I.I. Esakov, L.P. Grachev, K.V. Khodataev, A.A. Ravaev, and I.B. Matveev, "Investigations of Subcritical Streamer Microwave Discharge in Reverse-Vortex Combustion Chamber," IEEE Trans. Plasma Sci. Vol. 37, pp. 2293-2297, 2009.

[6] S. Takamura, S. Amano, T. Kurata, H. Kasada, J. Yamamoto, M.A. Razzak, G. Kushida, N. Ohno, and M. Kando, "Formation and decay processes of Ar/He microwave plasma jet at atmospheric gas pressure," J. Appl. Phys. Vol. 110, pp. 043301 (1-8), 2011.

[7] J.T. Krile, A.A. Neuber, H.G. Krompholz, and T. L. Gibson, "Monte Carlo simulation of high power microwave window breakdown at atmospheric conditions," Appl. Phys. Lett. Vol. 89, pp. 201501 (1-3), 2006.

[8] S.P. Kuo, Y.S. Zhang, M.C. Lee, P. Kossey, and R.J. Barker, "Laboratory chamber experiments exploring the potential use of artificially ionized layers of gas as a Bragg reflector for over-the-horizon signals," Radio Sci. Vol. 27, pp. 851-865, 1992.

[9] M. Baeva, H. Gier, A. Pott, J. Uhlenbusch, J. Hoschele, and J. Steinwandel, "Pulsed microwave discharge at atmospheric pressure for NO_x decomposition," Plasma Sources Sci. Technol. Vol. 11, pp. 1-9, 2002.

[10] A.V. Gurevich, N.D. Borisov, and G.M. Milikh, *Physics of Microwave Discharge: Artificially Ionized Regions in the Atmosphere (Gordon and Breach Science Publishers)*, The Netherlands, 1997.

[11] A.V. Gurevich, A.G. Litvak, A.L. Vikharev, O.A. Ivanov, N.D. Borisov, and K.F. Sergeichev, "Artificially ionized region as a source of ozone in the stratosphere," Phys.-Uspekhi Vol. 43, pp. 1103-1123, 2000.

[12] A.L. Vikharev, O.A. Ivanov, and A.G. Litvak, "Nonequilibrium Plasma Produced by microwave Nanosecond Radiation: Parameters, Kinetics, and Practical Applications," IEEE Trans. Plasma Sci. Vol. 24, pp. 460-477, 1996.

[13] J.H. Yee, R.A. Alvarez, D.J. Mayhall, D.P. Byrne, and J. Degroot, "Theory of intense electromagnetic pulse propagation through the atmosphere," Phys. Fluids, Vol. 29, pp. 1238-1244, 1986.

[14] J.H. Yee, D.J. Mayhall, G.E. Sieger, and R.A. Alvarez, "Propagation of Intense Microwave Pulses in Air and in a Waveguide," IEEE Trans. Antennas Propag. Vol. 39, pp. 1421-1427, 1991.

[15] Y. Hidaka, E.M. Choi, I. Mastovsky, M.A. Shapiro, J.R. Sirigiri, and R.J. Temkin, "Observation of Large Arrays of Plasma Filaments in Air Breakdown by 1.5-MW 110-GHz Gyrotron Pulses," Phys. Rev. Lett. Vol. 100, pp. 035003 (1-4), 2008.

[16] S.K. Nam and J.P. Verboncoeur, "Theory of Filamentary Plasma Array Formation in Microwave Breakdown at Near-Atmospheric Pressure," Phys. Rev. Lett. Vol. 103, pp. 055004 (1-4), 2009.

[17] J.P. Boeuf, B. Chaudhury, and G.Q. Zhu, "Theory and Modeling of Self-Organization and Propagation of Filamentary Plasma Arrays in Microwave Breakdown at Atmospheric Pressure," Phys. Rev. Lett. Vol. 104, pp. 015002 (1-4), 2010.

[18] B. Chaudhury and J.P. Boeuf, "Computational Studies of Filamentary Pattern Formation in a High Power Microwave Breakdown Generated Air Plasma," IEEE Trans. Plasma Sci. Vol. 38, pp. 2281-2288, 2010.

[19] B. Chaudhury, J.P. Boeuf, and G.Q. Zhu, "Pattern formation and propagation during microwave breakdown," Phys. Plasmas, Vol. 17, pp. 123505 (1-11), 2010.

[20] B. Chaudhury, J.P. Boeuf, and G.Q. Zhu, and O. Pascal, "Physics and modelling of microwave streamers at atmospheric pressure," J. Appl. Phys. Vol. 110, pp. 113306 (1-8), 2011.

[21] A. Cook, M. Shapiro, and R. Temkin, "Pressure dependence of plasma structure in microwave gas breakdown at 110 GHz," Appl. Phys. Lett. Vol. 97, pp. 011504 (1-3), 2010.

[22] A.M. Cook, J.S. Hummelt, M.A. Shapiro, and R.J. Temkin, "Observation of plasma array dynamics in 110 GHz millimeter-wave air breakdown," Phys. Plasmas, Vol. 18, pp. 100704 (1-4), 2011.

[23] K. Kourtzanidis, J.P. Boeuf, and F. Rogier, "Three dimensional simulations of pattern formation during high-pressure, freely localized microwave breakdown in air," Phys. Plasmas, Vol. 21, pp. 123513 (1-8), 2014.

[24] D.Z. Pai, D.A. Lacoste, and C.O. Laux, "Nanosecond repetitively pulsed discharges in air at atmospheric pressure—the spark regime," Plasma Sources Sci. Technol. Vol. 19, pp. 065015 (1-10), 2010.

[25] D.Z. Pai, "Nanomaterials synthesis at atmospheric pressure using nanosecond discharges," J. Phys. D: Appl. Phys. Vol. 44, pp. 174024 (1-7), 2011.

[26] A. Montello, D. Burnette, M. Nishihara, W.R. Lempert, and I.V. Adamovich, "Dynamics of Rapid Localized Heating in Nanosecond Pulse Discharges for High Speed Flow Control," J. Fluid Sci. Technol. Vol. 8, pp. 147-159, 2013.

[27] G.V. Naidis, "Simulation of spark discharges in high-pressure air sustained by repetitive high-voltage nanosecond pulses," J. Phys. D: Appl. Phys. Vol. 41, pp. 234017 (1-8), 2008.

[28] G. Sary, G. Dufour, F. Rogier, and K. Kourtzanidis, "Modeling and Parametric Study of a Plasma Synthetic Jet for Flow Control," Am. Inst. Aeronaut. Astronaut. (AIAA) J. Vol. 52, pp. 1591-1603, 2014.

[29] S.M. Starikovskaia, "Plasma assisted ignition and combustion," J. Phys. D: Appl. Phys. Vol. 39, pp. R265-R299, 2006.

[30] D.V. Roupassov, A.A. Nikipelov, M.M. Nudnova and A.Y. Starikovskii, "Flow Separation Control by Plasma Actuator with Nanosecond Pulsed-Periodic Discharge," Am. Inst. Aeronaut. Astronaut. (AIAA) J. Vol. 47, pp. 168-185, 2009.

[31] A. Yu. Starikovskii, A.A. Nikipelov, M.M. Nudnova, and D.V. Roupassov, "SDBD plasma actuator with nanosecond pulse-periodic discharge," Plasma Sources Sci. Technol. Vol. 18, pp. 034015 (1-17), 2009.

[32] K. Kourtzanidis, F. Rogier, and J.P. Boeuf, "Gas heating effects on the formation and propagation of a microwave streamer in air," J. Appl. Phys. Vol. 118, pp. 103301 (1-9), 2015.

[33] S.C. Schaub, J.S. Hummelt, W.C. Guss, M.A. Shapiro, and R.J. Temkin, "Electron density and gas density measurements in a millimeter-wave discharge," Phys. Plasmas, Vol. 23, pp. 083512 (1-8), 2016.

[34] I. Shkurenkov and I.V. Adamovich, "Energy balance in nanosecond pulse discharges in nitrogen and air," Plasma Sources Sci. Technol. Vol. 25, pp. 015021 (1-12), 2016.

[35] N.A. Popov, "Investigation of the Mechanism for Rapid Heating of Nitrogen and Air in Gas Discharges," Plasma Phys. Rep. Vol. 27, pp. 886-896, 2001.

[36] N.A. Popov, "Kinetic Processes Initiated by a Nanosecond High-Current Discharge in Hot Air," Plasma Phys. Rep. Vol. 37, pp. 807-815, 2011.

[37] N.A. Popov, "Fast gas heating in a nitrogen–oxygen discharge plasma: I. Kinetic mechanism," J. Phys. D: Appl. Phys. Vol. 44, pp. 285201 (1-16), 2011.

[38] N.A. Popov, "Pulsed nanosecond discharge in air at high specific deposited energy: fast gas heating and active particle production," Plasma Sources Sci. Technol. Vol. 25, pp. 044003 (1-17), 2016.

[39] A. Komuro and R. Ono, "Two-dimensional simulation of fast gas heating in an atmospheric pressure streamer discharge and humidity effects," J. Phys. D: Appl. Phys. Vol. 47, pp. 155202 (1-13), 2014.

[40] N.L. Aleksandrov, S.V. Kindusheva, M.M. Nudnova, and A.Y.U. Starikovskiy, "Mechanism of ultra-fast heating in a non-equilibrium weakly ionized air discharge plasma in high electric fields," J. Phys. D: Appl. Phys. Vol. 43, pp. 255201 (1-19), 2010.

[41] D.L. Rusterholtz, D.A. Lacoste, G.D. Stancu, D.Z. Pai, and C.O. Laux, "Ultrafast heating and oxygen dissociation in atmospheric pressure air by nanosecond repetitively pulsed discharges," J. Phys. D: Appl. Phys. Vol. 46, pp. 464010 (1-21), 2013.

[42] E.I. Mintoussov, S.J. Pendleton, F.G. Gerbault, N.A. Popov, and S.M. Starikovskaia, "Fast gas heating in nitrogen–oxygen discharge plasma: II. Energy exchange in the afterglow of a volume nanosecond discharge at moderate pressures," J. Phys. D: Appl. Phys. Vol. 44, pp. 285202 (1-13), 2011.

[43] A. Lo, G. Cleon, P. Vervisch, and A. Cessou, "Spontaneous Raman scattering: a useful tool for investigating the afterglow of nanosecond scale discharges in air," Appl. Phys. B, Vol. 107, pp. 229–242, 2012.

[44] A. Lo, A. Cessou, P. Boubert, and P. Vervisch, "Space and time analysis of the nanosecond scale discharges in atmospheric pressure air: I. Gas temperature and vibrational distribution function of N_2 and O_2," J. Phys. D: Appl. Phys. Vol. 47, pp. 115201 (1-14), 2014.

[45] S. Lanier, I. Shkurenkov, I.V. Adamovich, and W.R. Lempert, "Two-stage energy thermalization mechanism in nanosecond pulse discharges in air and hydrogen–air mixtures," Plasma Sources Sci. Technol. Vol. 24, pp. 025005 (1-13), 2015.

[46] A. Roettgen, I. Shkurenkov, M.S. Simeni, V. Petrishchev, I.V. Adamovich, and W.R. Lempert, "Time-resolved electron density and electron temperature measurements in nanosecond pulse discharges in helium," Plasma Sources Sci. Technol. Vol. 25, pp. 055009 (1-13), 2016.

[47] N.D. Lepikhin, N.A. Popov, and S.M. Starikovskaia, "Fast gas heating and radial distribution of active species in nanosecond capillary discharge in pure nitrogen and $N_2:O_2$ mixtures," Plasma Sources Sci. Technol. Vol. 27, 055005 (1-18), 2018.

[48] A. Flitti and S. Pancheshnyi, "Gas heating in fast pulsed discharges in N_2-O_2 mixtures," Eur. Phys. J. Appl. Phys. Vol. 45, pp. 21001 (1-7), 2009.

[49] V. Guerra and J. Loureiro, "Self-consistent electron and heavy-particle kinetics in a low-pressure N_2-O_2 glow discharge," Plasma Sources Sci. Technol. Vol. 6, pp. 373–385, 1997.

[50] C.D. Pintassilgo, V. Guerra, O. Guaitella, and A. Rousseau, "Study of gas heating mechanisms in millisecond pulsed discharges and afterglows in air at low pressures," Plasma Sources Sci. Technol. Vol. 23, pp. 025006 (1-19), 2014.

[51] C.D. Pintassilgo and V. Guerra, "On the different regimes of gas heating in air plasmas," Plasma Sources Sci. Technol. Vol. 24, pp. 055009 (1-15), 2015.

[52] C.D. Pintassilgo and V. Guerra, "Power Transfer to Gas Heating in Pure N_2 and in N_2-O_2 Plasmas," J. Phys. Chem. C, Vol. 120, pp. 21184−21201, 2016.

[53] S. Biabani and G. Foroutan, "Self consistent multi-fluid FDTD simulations of a nanosecond high power microwave discharge in air," Phys. Lett. A, Vol. 382, pp. 2720-2731, 2018.

[54] See http://www.lxcat.laplace.univ-tlse.fr to access BOLSIG+, which is a free software for numerical solution of the Boltzmann equation for electrons in weakly ionized gases.

[55] I.A. Kossyi, A. Yu. Kostinsky, A.A. Matveyev, and V.P. Silakov, "Kinetic scheme of the non-equilibrium discharge in nitrogen-oxygen mixtures," Plasma Sources Sci. Technol. Vol. 1, pp. 207-220, 1992.

[56] M. Capitelli, C.M. Ferreira, B.F. Gordiets, and A.I. Osipov, *Plasma Kinetics in Atmosphere Gases*, Springer, Berlin, 2000.

Gholamreza Foroutan received the B.Sc. and M.Sc. degrees in Physics from the University of Tabriz, Iran in 1996 and 1999, respectively. He obtained his Joint Ph.D. from Tabriz University, Iran and Sydney University, Australia in 2005. Currently, he is a Professor of Plasma Physics at Sahand University of Technology, Tabriz, Iran.

Samaneh Biabani received her B.Sc degree in Atomic and Molecular Physics from Urmia University, Iran in 2010 and M.Sc. degree in Plasma Physics from the University of Tabriz, Iran in 2013. She is a Ph.D. candidate of Plasma Physics at Sahand University of Technology, Tabriz, Iran, under supervision of Professor Foroutan.